Accepted for presentation in: IEEE International Symposium on Measurements and Networking (M&N), Rome, Italy, July 2024.

Performance Evaluation of IRS-enhanced mmWave Connectivity for 6G Industrial Networks

M. Danger*, C. Arendt*, H. Schippers*, S. Böcker*, M. Muehleisen†, P. Becker†, J. B. Caro†, G. Gjorgjievska†, M. A. Latif†, J. Ansari†, N. Beckmann‡, N. König‡, R. Schmitt‡, and C. Wietfeld*

*Communication Networks Institute (CNI), TU Dortmund University, 44227 Dortmund, Germany
E-mail: {Marco.Danger, Christian.Arendt, Hendrik.Schippers, Stefan.Boecker, Christian.Wietfeld}@tu-dortmund.de
†Ericsson GmbH, 52134 Herzogenrath, Germany
E-mail: {Maciej.Muehleisen, Paul.Becker, Jordi.Biosca.Caro, Gorjana.Gjorgjievska, Mazen.Abdel.Latif, Junaid.Ansari}@ericsson.com
‡Fraunhofer Institute for Production Technology (IPT), 52074 Aachen, Germany
E-mail: {Niklas.Beckmann, Niels.Koenig, Robert.Schmitt}@ipt.fraunhofer.de

***Abstract*—Private networks are a key innovation in the ongoing 5G era and the anticipated 6G landscape. The utilization of mmWave spectrum shows great potential for improving reliability in mobile and mission-critical industrial applications. Despite promising advancements demonstrated in controlled labs, deploying mmWave networks poses technical challenges, especially in dense, metallic industrial environments. This highlights the critical need for industry stakeholders to overcome associated technical challenges, thereby ensuring that end-to-end performance meets tailored requirements. Facilitating the transition of laboratory-validated benchmarks into practical industrial environments, we deploy our *STING Network Companion* as a distributed *KPI Monitoring and Control System* in a large-scale industrial manufacturing environment. Our results confirm the robust performance of mmWave technology in large-scale industrial environments, providing reliable connectivity even in most NLOS conditions. In addition, the deployment of our passive Intelligent Reflecting Surface (IRS) solution HELIOS demonstrates significant improvements through strategic placement, restoring LOS performance in obstructed locations seamlessly and therefore proving its applicability to real-world industrial applications. Our study validates the promising potential of mmWave frequencies to address challenges in realistic environments, thereby supporting its further adoption in industrial applications.**

***Video Abstract*—Video abstract can be accessed on http://tiny.cc/IndustrialmmWave**

I. Introducing mmWave Communications in Challenging Industrial Environments

The potential offered by Millimeter-Wave (mmWave) frequencies due to the large available bandwidth has not been used in many areas to date. This is partly due to challenges posed by blockage in Frequency Range 2 (FR2) and lack of expertise in efficiently handling the former. To gather these experiences, it is necessary to challenge mmWave networks and thus test their application.

In this work, the performance of a non-public 5G Non-Standalone (NSA) mmWave network, deployed in an industrial indoor environment, is evaluated. Based on the Spatially distributed Traffic and Interference Generation (STING) concept [1], our so-called *STING Network Companion* is used to implement a *KPI Monitoring and Control System*. Its integration within an industrial environment is illustrated in Fig. 1. Here, mobile and static STING units are deployed to continuously measure distributed network key performance indicators (KPIs). This information is supplemented in the backend process by centralized metrics obtained directly from the baseband. The resulting database is utilized for mitigation and optimization strategies to continuously improve the network performance.

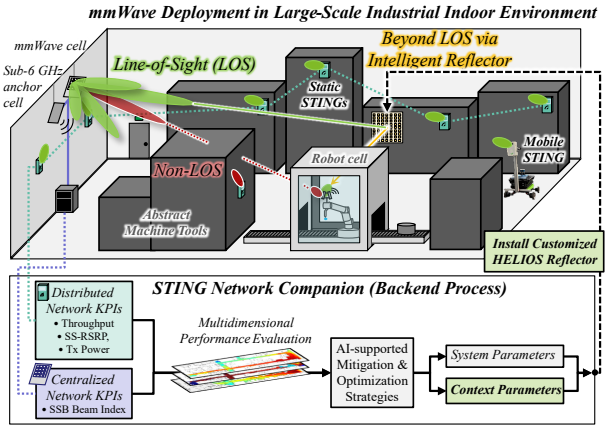

Fig. 1: Concept for continuous KPI monitoring and network optimization based on the *STING Network Companion*.

The measurements of [2] are extended to the size of a full-scale production facility to develop a proof-of-concept in a realistic environment based on the laboratory-validated feasibility study from the previous work. First, the baseline performance of the deployed network in Line-of-Sight (LOS) and Non-Line-of-Sight (NLOS) conditions is evaluated by mobile and static single-users. Afterward, the system's scalability is tested through multi-user measurements. Finally, with the help of a passive Intelligent Reflecting Surface, a so-called Holistic Enlightening of bLackspots with passIve reflectOr moduleS (HELIOS) reflector [3], a Beyond Line-of-Sight (BLOS) link is created seamlessly to realize improved connectivity in challenging areas. The results demonstrate the baseline performance of the mmWave network, its scalability for multi-users, and applicability of IRS-enhanced connectivity in large-scale industrial environments.

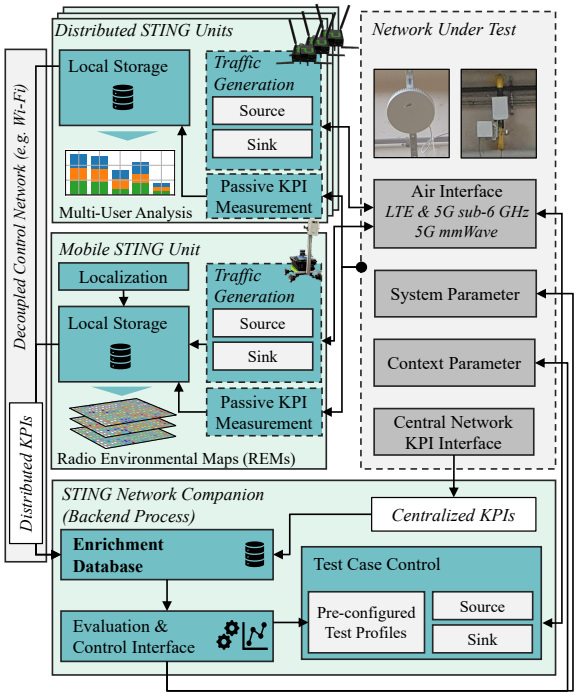

Fig. 2: Architecture overview of *STING Network Companion*.

The remainder of this work is structured as follows. In Sec. II the results of related studies are discussed. Sec. III describes the architecture and procedures for carrying out the intended measurements[1].The associated results are analyzed in Sec. IV to ultimately summarize the findings in Sec. V and give an outlook on our future projects.

II. Capabilities and Performance Evaluation of Indoor mmWave Networks

While this work focuses on achievable data rates as well as transmitted and received power in single- and multi-user scenarios, the performance of an indoor mmWave network can be evaluated under various aspects.

In [4] it is shown for mmWave and mid-band frequencies that latency requirements of industry applications can be fulfilled by 5G networks. The authors in [5] apply measurements from indoor and outdoor scenarios to predict the throughput of commercial mmWave 5G with the help of machine learning models. Findings of [6] show that the performance of industrial robotics systems in selected use cases is comparable when communicating via 5G mmWave or Ethernet. Furthermore, the authors suggest that concerns about challenges of mmWave frequencies are unwarranted as they can be compensated by other traits and technological advances. One of these technologies that can be used to improve FR2 radio coverage is IRS, cf. [7, 8]

Based on findings from our previous laboratory-validated results [2], we confirm the applicability and scalability of mmWave networks in industrial environments with the following experiments and show that optimization strategies can be successfully employed to improve performance in shadowed areas.

[1]Data at https://github.com/tudo-cni/TUDo-Industrial-mmWave-Dataset

III. Methodology for mmWave Performance Evaluation in Real-Life Industrial Environment

The methodology of this work is described in the following section. First, the architecture of the *STING Network Companion* is outlined in Sec. III-A. This is followed by an overview of the measurement scenarios within the production environment at Fraunhofer Institute for Production Technology (IPT) in Sec. III-B. Last, the metrics used for subsequent evaluations are outlined in Sec. III-C.

A. STING Network Companion Architecture

The *STING Network Companion* allows continuous KPI monitoring as well as reproducible stress tests with regard to applications and networks. It consists of a central backend process and multiple static as well as mobile decentralized STING modules, as depicted in Fig. 2.

The STING units are equipped modularly with different network modules to allow technology-independent testing, as well as providing a decoupled control channel over another network technology not tested in parallel. The monitored network KPIs are stored in a database for enrichment data within the *STING Network Companion*, allowing detailed performance evaluation and educated reconfiguration of system and context parameters of the network under test, e.g. enhancing coverage by installing IRSs. Distributed network KPIs can be augmented with centralized KPIs from the network under test, e.g. cell resource utilization and mmWave beam management information, to generate a holistic network performance overview. In this work, the presented architecture is used to evaluate the performance of an industrial NSA 5G system whose configuration is depicted in TABLE I. To ensure that data within the network is only transmitted via the FR2 component, the Long Term Evolution (LTE) and 5G Carrier Aggregation (CA) is disabled.

B. Measurement Scenarios in Industrial Environment

To provide an overview of the industrial indoor environment, the floor plan is shown in Fig. 3. In addition to the numbered positions 1 to 15 for static STING units, the route followed by the *Mobile STING* is marked. The latter has been developed to measure the 5G FR2 connectivity in large-scale industrial environments using a potent Light Detection and Ranging (LiDAR) sensor in conjunction with wheel odometry and Inertial Measurement Unit (IMU) data powered by *ROS 2*. As the *Mobile STING* platform is equipped with omnidirectional wheels, precise navigation and even a constant orientation of the attached FR2 modem are possible. All STING devices, both static on a tripod and mobile on the *Mobile STING*, are mounted at a height of 1.5 m. Furthermore, the position of the FR1 and FR2 cells is marked, which are wall-mounted at a height of 6 m. Based on this position, the LOS and NLOS areas for the main corridors within the scenario are marked. Also, a closable robot cell is highlighted, which is used together with a HELIOS reflector to investigate the IRS-enhanced connectivity under NLOS conditions. Utilizing the depicted environment, five different measurement setups have been developed, which challenge the mmWave connectivity in different ways:

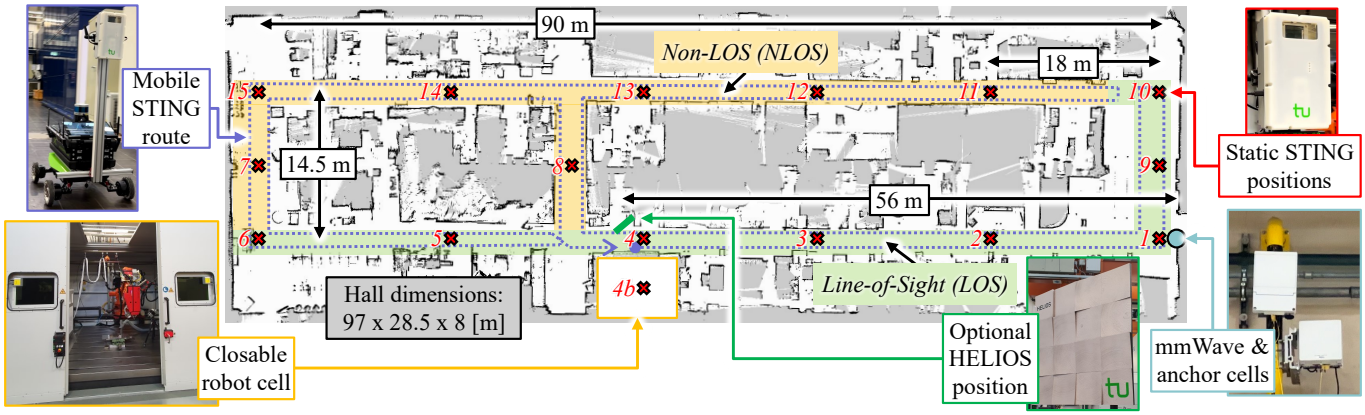

Fig. 3: Floor plan of industrial indoor environment with indicated positions of STINGs and measurement equipment for hands-on performance evaluation.

- *Mobile Single-User*: one STING device is attached to the *Mobile STING* for recording large-area Radio Environmental Maps (REMs).
- *Static Single-User*: one STING unit at a time is placed at one of the static positions with the respective antenna arrays horizontally aligned to the mmWave cell.
- *Co-Located*: three static STINGs are placed at the same location (orthogonally to the mmWave cell), whereby the following positions are considered: 2, 4, 6, 8 and 15
- *Mixed-Distance*: three static STINGs are positioned at different distances from the mmWave cell. Following position combinations are used: 2, 4, 6, and 2, 8, 15.
- *IRS-enhanced Single-User*: a static STING is placed inside the closable robot cell at position 4b with an optional HELIOS placed across the corridor.

TABLE I: Configuration of deployed elements in 5G NSA mobile network.

	Parameter	Description/Value
Cell Configuration	**FR1 / LTE Anchor Cell**	
	Radio Unit	Ericsson Radio 2203
	Frequency Band	LTE band 7 (FDD)
	Center Frequency	2.65 and 2.53 GHz (DL/UL)
	Bandwidth	5 MHz
	Transmit Power	5 W (EIRP)
	FR2 / NR mmWave Cell	
	Radio Unit	Ericsson AIR 1281
	Frequency Band	5G NR n257 (TDD)
	Frequency Range	26.7 to 27.5 GHz
	TDD Pattern	DDSU
	TDD Special Slot Pattern	11:3:0
	Component Carriers (CCs)	8
	Bandwidth	100 MHz per CC
	Subcarrier Spacing (SCS)	120 kHz
	Transmit Power	2 W (EIRP)
End Device	Number of Active Devices	up to three User Equipments (UEs)
	Device Model	Quectel 5GDM01EK with Quectel RG530F-EU
	Modem	Qualcomm SDX65
	mmWave Antenna Module	RA530T with four QTM547 (8×8, cross-polarized)
	LTE Category	Cat 20 / Cat 18 (DL/UL)
	5G NR Compliance	Release 16 NSA/SA
	Power Class	Class 3 (23 dBm)
	MIMO Capabilities	FR1: DL 4×4, UL 2×2 FR2: DL 2×2, UL 2×2
	IRS / HELIOS Reflector	Detailed design parameters in [2]

The installed HELIOS reflector [3] is a passive IRS consisting of 4×4 modules with a total size of $40\,\mathrm{cm} \times 40\,\mathrm{cm}$. As the reflector deployed in this work has already been used in the previous feasibility study, the detailed design parameters are provided in [2].

The shopfloor of IPT in Aachen, Germany features over 50 machine tools in various sizes on approx. 2,700 m^2 and therefore represents a realistic large-scale industrial indoor manufacturing environment. Its installed 5G mmWave cell is part of the 5G Industry Campus Europe (5G ICE). In preparation for the measurements carried out in the production hall, provided floor plans and photographs are utilized to derive a Digital Twin (DT). The latter is incorporated into *Wireless InSite* ray-tracing simulations together with antenna characteristics to calculate and visualize the expected radio propagation. The resulting simulated REM is compared and discussed with the measurement results (see also Fig. 4) in the subsequent section IV-A.

C. STING and Network Performance KPIs

While the listed measurements are performed, both STING and network KPIs are captured and merged in the *STING Network Companion*. To retrieve information from the STING units, specific *AT commands* are executed periodically using scripts to output passive metrics such as Synchronization Signal RSRP (SS-RSRP) as well as active KPIs, e.g., User Datagram Protocol (UDP) throughput via *iperf3*, utilized Modulation and Coding Scheme (MCS) and transmission power of the modem. On the network side, baseband information is queried at 1 s intervals. Among these are, for example, the Synchronization Signal Block (SSB) beam index (1 to 12) used by the mmWave cell and the Physical Resource Block (PRB) utilization (in 5 % steps).

When performing mobile measurements, the *Mobile STING* locates itself on a previously mapped floor plan of the industrial environment, as shown in Fig. 3. After one drive-through, area-wide REMs are created by linear spatial averaging over the recorded measurements, omitting areas where no measurements were taken. For the beam index REM, clustering is performed with *Voronoi* cells, as these indices are fixed values.

IV. Hands-On Evaluation of Indoor mmWave Network in Challenging Radio Conditions

This section covers the evaluation and analysis of the conducted measurements. First, the performance of a single mobile and static STING is examined in Sec. IV-A. The scalability is then evaluated in Sec. IV-B using different multi-user setups. Finally, in Sec. IV-C a passive IRS/HELIOS is introduced into the industrial environment to improve the performance in challenging NLOS conditions in an energy-efficient way.

A. Mobile & Static Single-user mmWave Connectivity

For measuring the baseline performance of the network without competing devices, the setups *Static Single-User* and *Mobile Single-User* are used. It should be noted that the throughput of each end device deployed is limited to a maximum of 2 Gbit/s for all subsequent measurements, as the devices would otherwise deliver highly fluctuating measured values. Since the employed end devices only support 400 MHz transmission bandwidth and a Downlink (DL)-heavy Time Division Duplex (TDD) pattern in configured (cf. TABLE I), the Uplink (UL) throughput is expected to be lower than in DL direction. The results of the mobile measurements are discussed first, followed by the static measurements.

In the top two images of Fig. 4, the simulated SS-RSRP is compared with the measured values. Both REMs are limited to the area in which measured values were captured without disconnections, which can occur due to the *Mobile STING's* mobility direction and speed. The comparison shows that the highest received power is approximately 6 m in front of the mmWave cell, which is due to its directionality and slight tilt. Along the horizontal, southern main corridor, the received power is comparatively high due to LOS conditions, although a decline is noticeable with increasing distance to the cell. North of the mmWave cell, high SS-RSRP values are simulated and measured due to reflections and beamsteering functionalities of the cell. In NLOS areas, significant performance drops

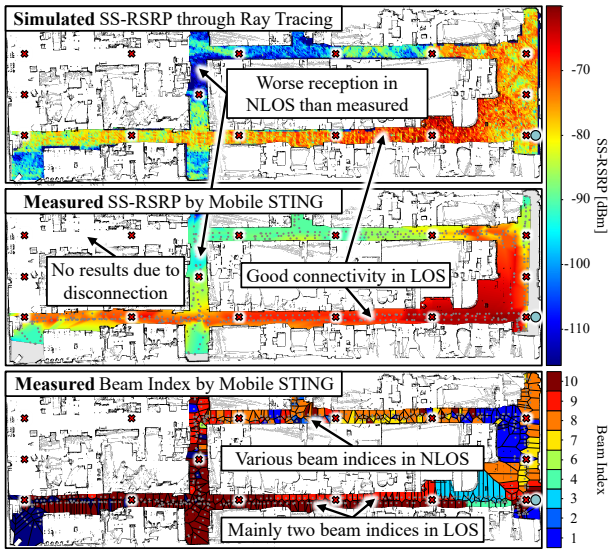

Fig. 4: Comparing simulation results and measured values by *Mobile STING*: simulated (*top*) and measured (*center*) SS-RSRP REMs as well as measured beam index REM (*bottom*).

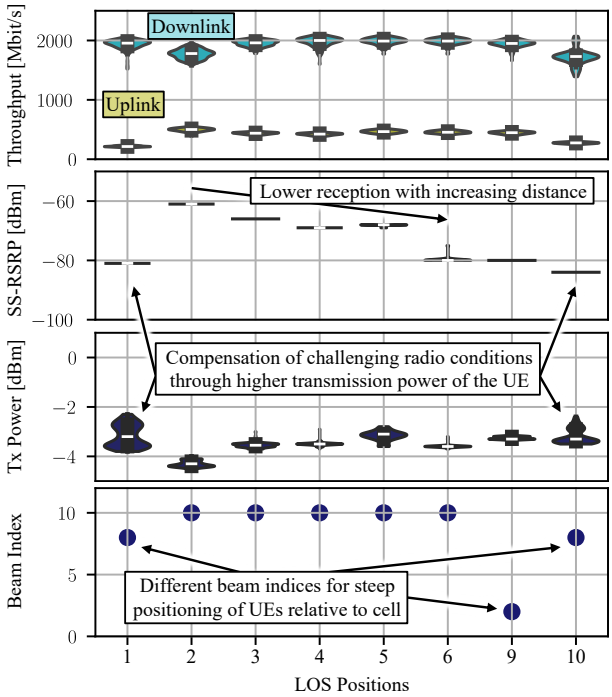

Fig. 5: Performance evaluation of Static STINGs in **LOS** conditions.

are evident, although these can be partially compensated by multipath propagation. There are obvious differences between reality and simulation in these areas, as the DT of the industrial environment only has a limited level of detail to limit the simulation time. Therefore, not all propagation paths that, in reality, lead to improved received power values can be mapped, as the measured SS-RSRP REM from *Mobile STING* shows.

The beam index REM reveals the utilization of multiple beams to reach the *Mobile STING* at various locations throughout the production hall. Along the southern main aisle, beam indices 9 and 10 are used for the most part. Near the cell and in NLOS areas, the REM is highly fragmented due to limitations of beamsteering and multipath propagation. Based on the metallic environment, it is assumed that the cell continuously discovers new reflection paths in these areas, which leads to a rapid change in measured beam indices.

In Fig. 5, the single-user performance in LOS conditions is evaluated based on throughput, SS-RSRP, transmission power of the STING unit, and beam index. The results show that the SS-RSRP, on average, is lowest at positions (pos.) 1 (−81.0 dBm), 6 (−79.8 dBm), 9 (−80.0 dBm) and 10 (−84.0 dBm). At pos. 1, 9 and 10, this is due to steep angles between end device and the mmWave radio unit, which leads to both main lobes being misaligned so that an alternative reflection path is selected, which is confirmed by the different beam indices used. The lower received power at pos. 6 is due to the increased distance to the mmWave antenna, as the course of SS-RSRP values from pos. 2 to 6 confirms. However, the transmission power of the FR2 modem shows that deteriorated radio conditions are partially compensated by the automatic transmission power control of the unit. Therefore, a maximum throughput of 2 Gbit/s in DL and 595 Mbit/s in UL direction can be achieved at several positions.

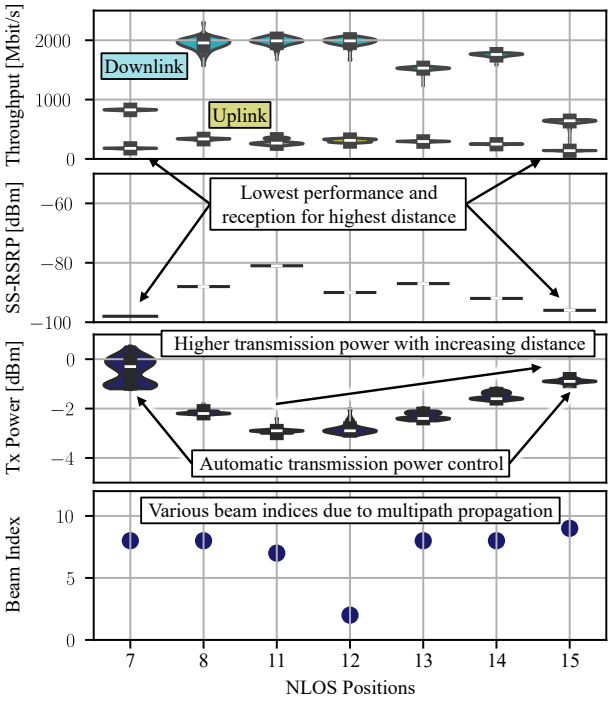

Fig. 6: Distributed and centralized networks KPIs of Static STINGs in **NLOS**.

Next, Fig. 6 analyzes the system performance at positions located in NLOS areas of the production hall. While connection interruptions occurred at pos. 7, 14 and 15 during the mobile measurements, the results indicate a successful completion in the static case, although the received power is comparatively poor. At pos. 7, the SS-RSRP is −98.0 dBm, whereby the throughput, on average, drops in UL to 178.2 Mbit/s, and in DL to 826.1 Mbit/s. These values are similar at pos. 15 with an SS-RSRP of −96.0 dBm, an average UL throughput of 137.7 Mbit/s, and 625.1 Mbit/s in DL. In contrast, with a 4 dB higher SS-RSRP (−92.0 dBm) and consequently higher MCS of 21 (instead of MCS 13 for pos. 7 and 15), a significantly higher DL throughput of, on average, 1.75 Gbit/s is achieved. This result underlines the impact a comparatively small improvement in connectivity can have on system performance. Furthermore, the analysis of further NLOS pos. shows that the transmission power of the STING unit rises with increasing distance and that various beams are utilized by the mmWave cell (indices 2, 7, 8 and 9).

B. Scalability Analysis for Multi-user Setups

Next, the scalability of the mmWave system is now examined in Fig. 7 using the multi-user setups *Co-Located* and *Mixed-Distance*. The results indicate an even distribution of the system's total throughput to the individual units in LOS conditions. In UL direction a maximum aggregated total throughput of 548.5 Mbit/s (approx. 182.8 Mbit/s per unit) is achieved, and in DL 3.63 Gbit/s (approx. 1.21 Gbit/s per unit). In contrast, the distribution is irregular if one or more STING units are located in NLOS areas. For example, the total throughput in the *Mixed-Distance* setup for position combination 2, 8, 15 is divided in DL (UL) direction as follows: 12 % (17 %) unit 3 at pos. 2, 34 % (31 %) unit 2 at pos. 8 and 54 % (52 %) unit 1 at pos. 15. Comparing the SS-RSRP values emphasizes the different radio conditions. The transmission power values illustrate the automatic counter-regulation of the units to achieve the highest possible throughput. The distribution of beam indices confirms findings from Sec. IV-A, showing that different beams are used to cover the measurement environment. These findings can be transferred to a lesser extent to the position combination 2, 4, 6, whereby the units are all located in LOS but are exposed to different radio conditions due to varying distances to the mmWave cell. Measurement results obtained in the *Co-Located* setup also confirm previous findings regarding the automatic transmission power control of the unit in worsened radio conditions (see pos. 6, 8 and 15) and rarely changing beam indices in LOS areas. In this setup, the measured values at pos. 6 are unexpected, as the three units in LOS measure different SS-RSRP values of up to 10 dB,

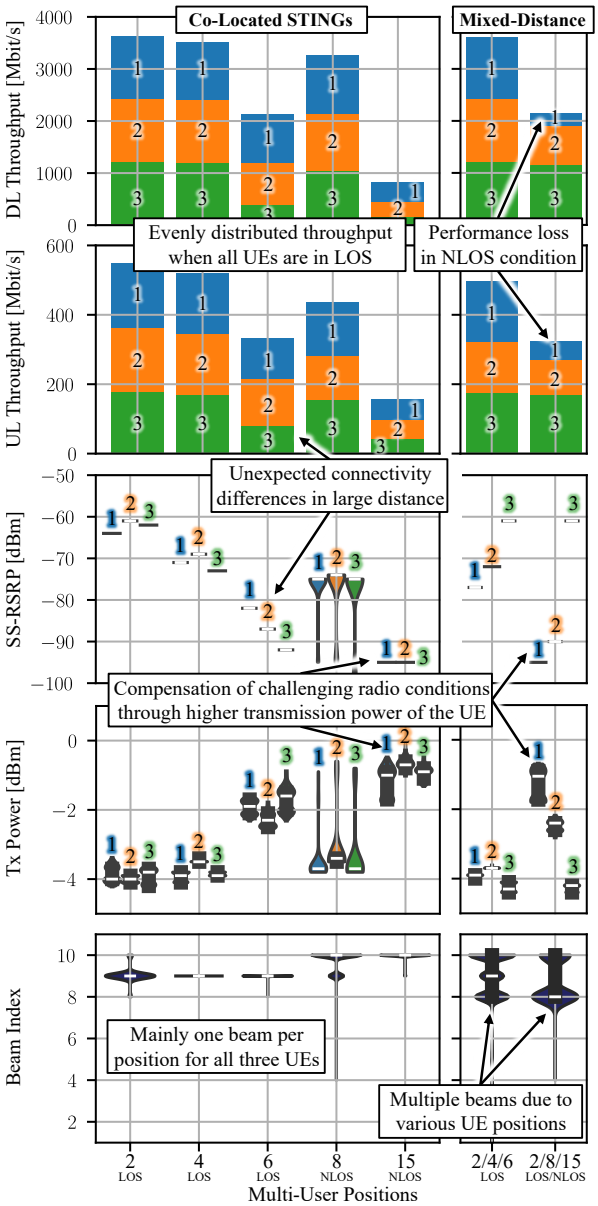

Fig. 7: Multi-user performance of static STINGs in Co-Located and Mixed-Distance setups under **LOS** and **NLOS** conditions.

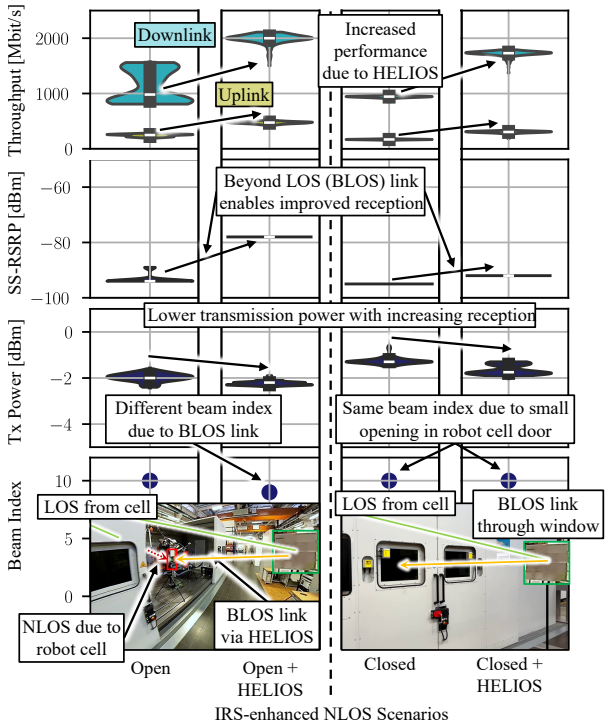

Fig. 8: Improving UE performance in challenging radio conditions by passive IRS/HELIOS creating a **BLOS** link.

which also leads to inconsistent throughput performances. The reason for these differences in performance may be due to unconsidered obstacles that affect the received power at the distance of 90 m between pos. 6 and mmWave cell.

C. Operation in OLOS/NLOS Regimes with IRS

Lastly, the performance of a single unit placed inside the closable robot cell at pos. 4b is investigated using the *IRS-enhanced Single-User* setup. The corresponding results are shown in Fig. 8. In the first scenario, the door of the metallic chamber is open. Both the measured throughputs and SS-RSRP show higher fluctuations than in previous measurements. This is due to the increased number of potential paths that exist between STING unit, an unspecific reflection surface, and the mmWave cell. When a HELIOS is now deployed in the second scenario, the reflector is seamlessly employed by the network and a BLOS link is created so that the distribution of the measured metrics is reduced. Furthermore, the performance at pos. 4b increases to a level comparable to pos. 4 in LOS: the throughput rises to 472.3 Mbit/s in UL and 1.98 Gbit/s in DL direction. At the same time, the transmission power of the unit decreases and a different beam index (index 9 instead of 10) is recorded. In the third scenario, the STING unit is inside the closed robot cell. Due to the strong shielding of the metallic chamber, the throughput in UL, on average, drops to 172.6 Mbit/s and in DL to 944.4 Mbit/s. The SS-RSRP is the lowest (−95.0 dBm), and the transmit power the highest (−1.27 dBm). The HELIOS reflector is deployed again in the fourth scenario, so that a BLOS link from the reflector, through the left window of the cell door to the STING unit is created. Its effect can be seen across the previously mentioned metrics: the UL (DL) throughput increases to 302.8 Mbit/s (1.72 Gbit/s), the SS-RSRP rises by 3 dB and the transmit power decreases by 0.37 dB. These results show that HELIOS reflectors can improve radio coverage and system performance even in large-scale industrial environments.

V. Conclusions and Outlook

In this work, we assessed the mobile and static baseline network performance in a large-scale industrial environment with the help of our *STING Network Companion*. Here, maximum data rates in LOS areas of 595 Mbit/s in UL and 2 Gbit/s in DL direction were achieved for single-users. In NLOS conditions, it became evident that performance drops were partially compensated by the transmission power control of the FR2 modems and that different beam indices were utilized by the mmWave cell to improve connectivity. The multi-user measurements performed confirmed the scalability of the network with evenly distributed throughputs in LOS conditions, aggregating to a maximum of 548.5 Mbit/s in UL and 3.63 Gbit/s in DL direction. The applicability of IRS-enhanced mmWave connectivity to real-world industrial environments was then demonstrated by improvements in performance as well as energy efficiency based on BLOS links via a HELIOS reflector that was seamlessly employed by the network without any reconfiguration. This underlines the great potential of passive IRSs for future 6G networks.

In our future work, we will deploy our *STING Network Companion* in different industrial environments, examine the energy consumption in more detail and continue to challenge the mmWave system with scaled multi-user tests as well as mobility. Furthermore, network planning algorithms are investigated to calculate the position of passive IRSs automatically.

Acknowledgment

This work has been funded by the German Federal Ministry of Education and Research (BMBF) in the course of the *6G-ANNA* project under grant no. 16KISK101 and the *6GEM Research Hub* under the grant no. 16KISK038 as well as by the Ministry of Economic Affairs, Industry, Climate Action, and Energy of the State of North Rhine-Westphalia (MWIKE NRW) along with the *Competence Center 5G.NRW* under grant no. 005-01903-0047.

References

[1] C. Arendt, M. Patchou, S. Böcker, J. Tiemann, and C. Wietfeld, "Pushing the limits: Resilience testing for mission-critical machine-type communication," in *Proc. IEEE VTC-Fall*, 2021.

[2] M. Danger, S. Häger, K. Heimann, S. Böcker, and C. Wietfeld, "Empowering 6G industrial indoor networks: Hands-on evaluation of IRS-enabled multi-user mmWave connectivity," in *Proc. EuCNC/6G Summit*, Jun. 2024.

[3] S. Häger, K. Heimann, S. Böcker, and C. Wietfeld, "Holistic enlightening of blackspots with passive tailorable reflecting surfaces for efficient urban mmWave networks," *IEEE Access*, vol. 11, 2023.

[4] J. Ansari, C. Andersson, P. de Bruin, J. Farkas, L. Grosjean, J. Sachs, J. Torsner, B. Varga, D. Harutyunyan, N. König, and R. H. Schmitt, "Performance of 5G trials for industrial automation," *Electronics*, vol. 11, no. 3, 2022.

[5] A. Narayanan, E. Ramadan, R. Mehta, X. Hu, Q. Liu, R. A. K. Fezeu, U. K. Dayalan, S. Verma, P. Ji, T. Li, F. Qian, and Z.-L. Zhang, "Lumos5G: Mapping and predicting commercial mmWave 5G throughput," in *Proc. ACM IMC*, Oct. 2020.

[6] V. Ayadurai, R. Narayanan, and B.-E. Olsson, "Experiments with industrial robotics systems over an indoor 5G-NSA mmWave deployment," in *Proc. EuCNC/6G Summit*, 2023.

[7] J.-B. Gros, V. Popov, M. A. Odit, V. Lenets, and G. Lerosey, "A reconfigurable intelligent surface at mmWave based on a binary phase tunable metasurface," *IEEE OJ-COMS*, vol. 2, 2021.

[8] R. Liu, J. Dou, P. Li, J. Wu, and Y. Cui, "Simulation and field trial results of reconfigurable intelligent surfaces in 5G networks," *IEEE Access*, vol. 10, 2022.